ACS NANOSCIENCE Au
AN OPEN ACCESS JOURNAL OF THE AMERICAN CHEMICAL SOCIETY

pubs.acs.org/nanoau
Article

Enhanced Anti-Inflammatory and Skin Barrier Repair Effects of Nanoemulsions Supplemented with *Boesenbergia rotunda* for Atopic Dermatitis

Desy Liana, Jaruwan Chatwichien, and Anuchit Phanumartwiwath*

Cite This: *ACS Nanosci. Au* 2025, 5, 37−51
Read Online

ABSTRACT: Betamethasone dipropionate (BD) is a potent anti-inflammatory drug for atopic dermatitis (AD); however, it leads to serious adverse effects during prolonged use. We aimed to improve the biochemical properties and lower the risk of toxicity by preparing nanoemulsions containing *Boesenbergia rotunda* rhizome hexane extract (Hex) and essential oils (EO). Physicochemical characterization and 3-month long-term stability testing were conducted. Gas chromatography−mass spectrometry analysis was used to compare the volatile composition after nanoemulsion formulation. Further, various assays related to AD management, including antioxidant potentials, anti-inflammatory activities through inhibition of 5-lipoxygenase and cyclooxygenase-2, and nitric oxide release suppression in lipopolysaccharides-induced RAW 264.7 macrophages, were investigated. In addition, antibacterial activity against *Staphylococcus aureus* and cytotoxicity to RAW 264.7 macrophages and HaCaT human keratinocyte cells were also evaluated. Monodispersed nanoemulsions (<20 nm) were successfully generated by an ultrasound-assisted method. BD was successfully encapsulated into *B. rotunda*-based nanoemulsions with more than 95% encapsulation efficiency (EE). The major phytochemicals present in EO and Hex remained after nanoemulsion formulation. The nanoemulsions were compatible with skin pH (5.2−5.8) and exhibited stability with respect to particle size, polydispersity index, transmittance, pH, and EE when stored for 3 months at −20 °C. The BD nanoemulsions loaded with *B. rotunda* exhibited antioxidant activities and significantly increased the 5-lipoxygenase inhibitory activity. Furthermore, the suppression of nitric oxide release was remarkably enhanced, whereas lower cytotoxicity was observed. The BD nanoemulsions improved the level of involucrin and filaggrin in HaCaT cells, implying their valuable property for skin barrier repair. The formulation of BD into nanoemulsions also enhanced *S. aureus* inhibition. Either *B. rotunda* nanoemulsions loaded with or without BD show promise for the topical treatment and prevention of AD.

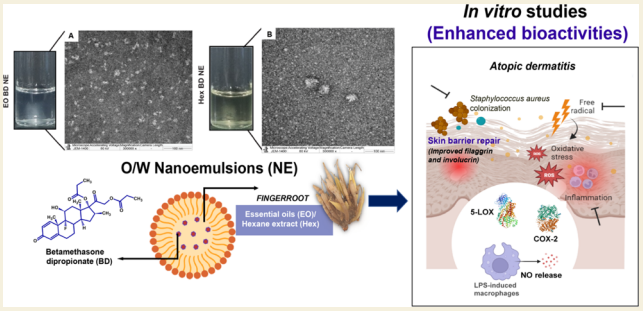

KEYWORDS: *pinostrobin, nanomedicine, betamethasone dipropionate, inflammation, skin barrier, atopic dermatitis*

INTRODUCTION

Betamethasone dipropionate (BD), a high-potency topical corticosteroid, is used for the treatment of severe and refractory atopic dermatitis (AD).[1] It suppresses inflammation by targeting phospholipase A2 in the arachidonic acid pathway.[2,3] A lack of water and sodium retention is the major advantage of BD compared with other corticosteroids;[4] however, it has poor skin permeability. In addition, despite its effectiveness, prolonged use can cause serious local and systemic side effects (e.g., Cushing syndrome, growth retardation, epidermal thinning, facial erythema, rosacea, glaucoma, cataract, blindness, alopecia, delayed wound healing, and hyperpigmentation).[5,6] Accordingly, alternative safer medications for long-term treatment are essentially needed. Herbal medicines offer a promising alternative, as they exhibit various pharmacological actions beneficial for suppressing AD symptoms.

Boesenbergia rotunda (L.) Mansfield, the fingerroot commonly used as a cooking spice in Asian countries,[7] exhibits anti-inflammatory and antibacterial properties. Traditionally, the rhizome of *B. rotunda* is used for treating dermatitis and wounds and relieving skin itchiness.[8,9] A previous study reported that an ethanol extract of rhizome attenuated AD in an in vivo model of skin barrier damage, including erythema, trans-epidermal water loss, and filaggrin expression.[10] Based on our previous study, we used *B. rotunda* exhibits promising properties, such as antioxidant and antibacterial against

Received: August 28, 2024
Revised: November 19, 2024
Accepted: November 20, 2024
Published: December 2, 2024

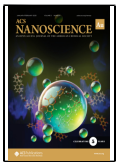

Table 1. Optimized Formula for Nanoemulsions[a]

formula	olive oils (% w/v)	*B. rotunda*-based oils (% w/v)		BD (% w/v)	ethanol (% v/v)	polysorbate-80 (% w/v)	glycerol (% v/v)	sonication (min)
		EO	Hex					
EO NE	1	0.5			1	9.375	5.2	30
Hex NE	1		0.5		1	9.375	5.2	60
EO BD NE	1	0.5		0.05	1	9.375	5.2	30
Hex NE BD	1		0.5	0.05	1	9.375	5.2	60
blank NE	1				1	9.375	5.2	30

[a]Ultrapure H_2O was added to obtain 100% final volume; BD = betamethasone dipropionate; EO = hydro-distilled essential oils; and Hex = hexane extract.

Staphylococcus aureus, and anti-inflammatory effects through 5-lipoxygenase (5-LOX) and cyclooxygenase-2 (COX-2) inhibition. 5-LOX and COX-2 play critical roles in mediating inflammation from arachidonic acid metabolism through the production of leukotrienes and prostaglandins that can exacerbate the AD symptoms.[11] This dual 5-LOX and COX-2 inhibitor may serve as a target for suppressing inflammation and pruritic symptoms in AD skin by inhibiting various proinflammatory cytokines involved in AD pathogenesis, such as leukotriene (LT) B4, prostaglandin (PG) D2, and PGE2.[12−15] Furthermore, Q301 (zileuton), a 5-LOX inhibitor, has entered a phase 2A clinical trial and improved AD skin lesions.[16] Macrophages accumulate in acute and chronically inflamed AD skin and act as a connecting center during the inflammation process.[17] The high amount of nitric oxide (NO) released in macrophages plays a role in recurrent chronic.[18] NO levels in AD patients were higher compared with those of controls.[19] Elevated levels of NO contribute to oxidative stress and sustain a prolonged state of skin inflammation.[20] A previous clinical study revealed that topical *N*-ω-nitro-L-arginine, a nitric oxide synthase inhibitor, reduced inflammation and skin symptoms in AD patients.[21] Moreover, decreased expression of barrier proteins such as filaggrin and involucrin were found in AD skin.[22] Keratinocytes produce filaggrin protein and play a role in the maintenance of moisture, pH, and skin protection from pathogens.[23] On the other hand, involucrin is known as an essential substrate for attachment of ceramides and cornified envelope in the epidermis.[24] Consequently, inhibition of the inflammatory response (NO release) caused by lipopolysaccharide (LPS) and improvement of barrier proteins, such as filaggrin and involucrin, may be effective strategies for AD treatment and prevention.

One strategy for lowering systemic side effects for topical applications is to improve drug retention and minimize the amount of drug entering the systemic circulation.[6] Nanoemulsions are considered the most translatable nano delivery systems and have been widely used for managing inflammatory skin diseases, including AD. This system is biocompatible and exhibits superior encapsulation of low water-soluble drugs to improve in vivo delivery. The ability of nanoemulsions to shield the loaded drug from enzymatic and chemical degradation, such as low pH, provides better therapeutic properties for the active compound, including a reduced effective concentration.[25,26] Oil-in-water (O/W) nanoemulsions offer high loading capacity for lipophilic drugs like BD, enhanced skin penetration due to their small particle size, and improved skin hydration, making them more advantageous for managing AD compared to lipid-based nanoformulations.[27,28] Nanoemulsion formulation can be performed with low- and high-energy methods.[29] Among the high-energy methods, the ultrasonication technique is regarded as the most efficient one, producing small droplets with a low polydispersity index while requiring low amounts of surfactant, energy consumption, and operating costs and applicable on both laboratory and industrial scales.[30,31]

As aforementioned, *B. rotunda* EO and hexane extracts are promising candidates for AD management. Therefore, we aimed to encapsulate BD into *B. rotunda* EO and hexane extract as a nanoemulsion assisted by the ultrasonication method and evaluate its antibacterial, antioxidant, and anti-inflammatory activities through 5-LOX, COX-2, and NO suppression in LPS-induced RAW 264.7 macrophage cells. Cytotoxicity against RAW 264.7 macrophages and HaCaT human keratinocyte cells related to AD pathology was also determined. Furthermore, the skin barrier repair property by determining involucrin and filaggrin expression was also investigated. Our main goal is to enhance the pharmacological efficacy of BD while reducing its dosage by formulating it into the nanoemulsion supplemented with *B. rotunda* extract or essential oils.

EXPERIMENTAL SECTION

Plant Material Preparation and Extraction

B. rotunda (L.) Mansf. rhizomes were collected from Bangkok, Thailand, in April 2022. These rhizomes were authenticated and deposited at the Department of Botany, Faculty of Science, Chulalongkorn University [Zingiberaceae; 17530 (BCU)]. The nonpolar fractions, including essential oils and hexane extract, were obtained by hydrodistillation and ultrasound-assisted extraction, respectively. Both extraction methods were conducted according to our previous method.[11] Briefly, essential oils were obtained through hydrodistillation by subjecting 100 g of fresh rhizome to the Clevenger apparatus, yielding 0.216%. The crude hexane extract was provided through using an ultrasound-assisted method by extracting 50 g of dried rhizome powder into 250 mL of hexane, resulting in a yield of 2.430%.

Nanoemulsion Formulation

Preparation of Oil-in-Water Nanoemulsions by the Ultrasound-Assisted Method. The oil phase containing olive oils, bioactive components (BD and EO or Hex), and polysorbate-80 was mixed with magnetic stirring at 250 rpm for 5 min. Afterward, the dropwise addition of ultrapure water containing glycerol was done while stirring at 500 rpm and continued for 30 min at 1000 rpm. To facilitate the droplet size reduction, we used the ultrasonication-assisted technique, which was adapted and modified from the previous study.[32] The emulsion was subjected to an ultrasonication bath at 35 kHz, 75% power, and 25 °C. The successive nanoemulsion formulation (with no phase separation after 24 h of observation) was subjected to further stability testing and characterization. The

https://doi.org/10.1021/acsnanoscienceau.4c00053
ACS Nanosci. Au 2025, 5, 37−51

optimized formulas obtained from the various conditions are listed in Table 1.

Stability Testing. Centrifugation, heating, cooling, and freeze−thaw cycles were performed based on previous studies[33,34] to evaluate destabilization phenomena. All formulas were centrifuged at 5000 rpm for 30 min. Only formulas with no destabilizing phenomena were selected for the heating and cooling testing. The preparation was subjected to six heating (40 °C) and cooling (4 °C) cycles for at least 48 h for each cycle. The stable formulas were then subjected to six freeze−thaw cycles. One cycle of freeze−thaw involved storage at −20 °C for 24 h and additional thawing at 25 °C (room temperature) for 24 h. The experiment was performed in triplicate. Only the formulas that passed the test were characterized and subjected to long-term storage stability testing. The long-term storage stability testing of the nanoemulsions was performed for 3 months. Encapsulation efficiency (EE) was determined on the day of formulation and 90 days postpreparation. The nanoemulsions were stored in a light-protected container at −20 ± 5 °C before further use.

Physicochemical Characterization of Nanoemulsions

Determination of Percentage Transmittance and pH. The transmittance of the nanoemulsions was determined using a UV−vis spectrophotometer (Shimadzu, UV-1800) at 600 nm, with ultrapure water serving as a blank. In addition, the pH values of the nanoemulsions were measured in triplicate at 25 °C by using a digital pH meter (PH700, APERA Instrument).

Particle Size, Polydispersity Index, and Zeta Potential Determination. The particle size and PDI measurements were performed at the Scientific and Technological Research Equipment Centre (STREC), Chulalongkorn University. Dynamic light scattering (DLS) using the MALVERN Zetasizer Nano ZSP was used to determine the mean average particle size (Z-Ave) and PDI at 25 °C. Polystyrene cells were used, and the measurements were conducted in triplicate.

Electrophoretic light scattering was used to measure the zeta potential. Measurements were performed at 25 °C with 0.15−0.17 mS/cm conductivity and ultrapure water as the dispersant. The Helmholtz−Smoluchowski equation was used to obtain the zeta potential value.

Transmission Electron Microscopy. The morphology of the nanoemulsions loaded with BD and EO/hexane extract was observed by transmission electron microscopy (TEM) (JEOL TEM-1400) at the STREC, Chulalongkorn University. After being diluted with ultrapure water (1:10), the samples were negatively stained with 1% uranyl acetate.

Encapsulation Efficiency. The nanoemulsion (0.5 mL) was ultracentrifuged at 10 000 rpm for 30 min using an Amicon ultra centrifugation filter with a 10 kDa molecular weight cutoff. To determine the unencapsulated BD in the water phase, the filtrate was analyzed using a Shimadzu reversed-phase high-performance liquid chromatography (RP-HPLC) LL-20A system equipped with a CMB-20A controller, SIL-20A autosampler, DGU-20A3 online degassing unit, and SPD-M20A photodiode array detector.

Chromatography separation was performed with a C_{18} column (4.6 mm × 250 mm) coupled to a C_{18} guard column (4.6 mm × 10 mm) as the stationary phase. Separation was done in an isocratic mode with 60% acetonitrile in ultrapure water for 30 min at 25 °C at a flow rate of 0.8 mL/min. BD was detected at 238 nm (RT = 22.09 min). The measurements were carried out in triplicate. The measurement of EE was performed using the following formula

$$\text{EE}\ (\%) = \frac{(\text{Wa} - \text{Ws})}{\text{Wa}} \times 100$$

where EE = encapsulation efficiency; Wa = amount of drug loaded in the formula; and Ws = amount of free drug in the water phase.

Gas Chromatography−Mass Spectrometry (GC−MS). A Finnigan Trace GC Ultra equipped with a Phenomenex Zebron ZC-5 MS capillary column (5% phenyl, 95% methyl poly siloxane, 30 m × 0.25 mm × 0.25 μm film thickness) and a DSQ quadrupole detector with electron impact (EI) ionization positive mode at 70 eV were used to analyze the volatile components present in EO, hexane extract, and nanoemulsions. The temperature of the EI ion source and injection port was maintained at 230 and 240 °C, respectively, whereas the column initial temperature was maintained at 60 °C for 3 min and then increased at 3 °C/min until it reached 240 °C. Helium (>99%) was used as a carrier gas at a flow velocity of 1 mL/s. Before sample injection, the volatile components of the nanoemulsions were extracted with chloroform. The samples (1 μL, 1 mg/mL in methanol) were injected using a Finnigan Autoinjector AI3000 with a split ratio of 1:10. The volatile components were identified by comparing their MS spectra with those of the NIST05 and Adams essential oil libraries. To determine the average percentage abundance, the samples were analyzed in triplicate. The percent abundance of the components was calculated using the area normalization method.

Antioxidant Determination

DPPH Radical Scavenging Activity. The EO and hexane extracts were each dissolved in DMSO, whereas the nanoemulsion was diluted in water. The samples (20 μL, 0.625−5 mg/mL) were placed into a 96-well plate, and 180 μL of 120 μM DPPH solution (in methanol) was added. Incubation was performed under dark conditions at 37 °C for 30 min. The absorbance was measured at 517 nm by using a microplate reader (BioTek Synergy H1, Agilent). Quercetin and the solvent were used as positive and negative controls, respectively. Radical scavenging (percentage of inhibition) against DPPH was determined by the following formula

$$\text{inhibition}(\%) = \frac{(\text{absorbance control} - \text{absorbance sample})}{\text{absorbance control}} \times 100$$

Nitric Oxide Radical Scavenging Activity. The Griess assay was used to determine NO radical scavenging activity using a procedure modified from our previous study.[11] EO and hexane extract were individually dissolved in DMSO, and the nanoemulsion was diluted in water. NO radicals were generated from sodium nitroprusside (SNP), pH 7.3, by incubating 10 μL of sample (0.625−2.5 mg/mL) with 90 μL of 10 mM SNP in phosphate-buffered saline (PBS) in a 96-well plate under visible polychromatic light at 250 rpm and 25 °C for 90 min. Next, 50 μL of 1% sulfanilamide (in 5% H_3PO_4) was added, and the reactions were incubated for 5 min in the dark at 25 °C and 250 rpm. After the addition of 50 μL of 0.1% *N*-(1-naphthyl)-ethylenediamine (NED) in H_2O, the samples were incubated for another 30 min under the same conditions. The diazotization of sulfanilamide with the nitrite ion was done, followed by a coupling reaction with NED to produce a pink chromophore (magenta). The absorbance was measured at 540 nm. Quercetin was used as a positive control, and solvent was used as a control blank. The amount of nitrite in the SNP-treated group was used as a control group to calculate the percentage of NO radical scavenging activities. The determination of the percentage inhibition was done using the following formula

$$\text{inhibition}\ (\%) = \frac{(\text{absorbance control} - \text{absorbance sample})}{\text{absorbance control}} \times 100$$

Ferric-Reducing Antioxidant Power. EO and hexane extract were individually dissolved in DMSO, whereas the nanoemulsion was diluted in water. Samples (10 μL, 1 mg/mL) were incubated with 190 μL of freshly prepared Ferric-reducing antioxidant power (FRAP) reagent in a 96-well plate at room temperature for 4 min. The reduction of ferrous ions into ferric ions generated an intense blue color, and the absorbance was measured at 595 nm. The concentration of ferric ions in the samples relative to the standard $FeSO_4$ (FRAP value in μM $FeSO_4$/mg dry weight of extract) based on a standard calibration curve was used to determine the antioxidant power using the FRAP value.

https://doi.org/10.1021/acsnanoscienceau.4c00053
ACS Nanosci. Au 2025, 5, 37−51

$$\text{FRAP value} = C \times \frac{V}{(\text{df} \times \text{cs})}$$

where C = calculated concentration obtained from the calibration curve, Vs = volume sample added in each well (mL), df = dilution factor, and cs = concentration of the sample used (mg/mL).

Antibacterial Assay against *S. aureus*. Minimum inhibitory concentration (MIC) was determined by using a broth dilution assay. The EO and extract dissolved in DMSO (0.2% v/v) were suspended in Lysogeny broth (LB) medium to obtain a final concentration of EO/extract, pinostrobin, and standard drug (tetracycline) in the range of 0.156−200 μg/mL. The bacterial culture (20 μL) at a 0.002 initial OD_{600} was further inoculated. The treated culture was then incubated at 37 °C and 180 rpm for 24 h. The absorbance was measured at 600 nm. LB medium and 0.2% DMSO were used as positive controls, whereas a cell culture without treatment in LB medium was used as a negative control. Tetracycline was used as the antibiotic standard. The experiments were performed in triplicate. The percentage of inhibition was determined relative to the OD_{600} of the negative control.

Anti-Inflammatory Assays

Cyclooxygenase-2 (COX-2) Inhibitory Assay. The COX-2 inhibitory assay was modified from a previous study.[35] Initially, 100 mM Tris HCl buffer (pH 8) was added to a plate, followed by the addition of 40 μL of sample (dissolved in polysorbate-20 and DMSO). Subsequently, 40 μL of 40 U human recombinant COX-2 (Sigma-Aldrich, C0858) in ice-cold 100 mM Tris HCl buffer, pH 8, was added, and the mixture was incubated for 15 min at 25 °C in the dark. Next, 10 μL of 20 mM *N*,*N*,*N*′,*N*′-tetramethyl-*p*-phenylenediamine (TMPD) and 10 μM of arachidonic acid (4 μL) were added, and the reactions were incubated under subdued light conditions for 15 min. The reaction produced prostaglandin G_2 (PGG_2) as an intermediate peroxide. Further oxidation of TMPD into a purple TMPD complex also occurred. Experiments were performed in duplicate, and the absorbance was measured at 611 nm. Diclofenac sodium was used as a positive control, whereas a solvent was used as a blank control. IC_{50} values were calculated after determining the percent inhibition.

$$\text{inhibition (\%)} = \frac{(\text{absorbance control} - \text{absorbance sample})}{\text{absorbance control}} \times 100$$

5-Lipoxygenase (5-LOX) Inhibitory Assay. This assay was performed based on a previous study,[36] with some modifications. Samples (20 μL) at various concentrations (dissolved in polysorbate-20 and DMSO) were added to a 96-well UV-transparent plate, followed by the addition of 0.1 M potassium phosphate buffer, pH 6.3 (100 μL). Before the addition of human recombinant 5-LOX (Cayman Chemical, E.C. 1.13.11.34), the mixture was kept at 25 °C. Subsequently, 20 μL of 100 U 5-LOX in 0.1 M potassium phosphate (PBS) buffer, pH 6.3, was added, and the mixture was incubated at 25 °C for 4 min. The reaction was initiated by the addition of 10 μL of 1 mM arachidonic acid as a substrate. The absorbance was measured with a microplate reader at 234 nm after a 30 min incubation at 25 °C. A nonenzymatic control was used for background correction, whereas nordihydroguaiaretic acid (NDGA) and BD were used as positive controls. Two independent experiments were conducted to generate five replicate wells. IC_{50} values were determined after calculating the percentage inhibition using the following equation

$$\text{inhibition (\%)} = \frac{(\text{absorbance control} - \text{absorbance sample})}{\text{absorbance control}} \times 100$$

Determination of NO Release Suppression in LPS-Induced RAW 264.7 Macrophages. The suppression of NO release in LPS-induced RAW 264.7 macrophage cells was determined using the previously described method.[37] RAW 264.7 (ATCC TIB-71) was obtained from Bimedia (Thailand) Co., Ltd. The cells were cultured in Dulbecco's modified Eagle's medium (DMEM, Gibco, Thermo Fisher Scientific, Inc.) supplemented with 10% fetal bovine serum (FBS, HyClone, USA), 100 U/mL penicillin−streptomycin (Gibco, Thermo Fisher Scientific, Inc.), and maintained at 37 °C, 5% CO_2, in humidified air. Briefly, 10^5 cells/well of macrophage cells were cultured in a 24-well plate for 24 h. The cells were then incubated with the tested samples (0.125−20 μg/mL) for 1 h prior to stimulation with 100 ng/mL LPS (Sigma-Aldrich cat. No. L4391−1). After 24 h of incubation, the NO levels were determined by the Griess assay. The culture medium (50 μL) was mixed with 50 μL of Griess reagent (Sigma-Aldrich cat. No. G4410) and incubated for 10 min, and the absorbance was measured at 540 nm. Bay 11−7082 (Sigma-Aldrich cat. No. B5556) was used as a positive control, and the solvent was used as a blank. The experiments were performed in triplicate.

Cytotoxicity of the Nanoemulsions against HaCaT Human Keratinocytes and RAW 264.7 Macrophages. The 3-(4,5-dimethylthiazol-2-yl)-2,5-diphenyltetrazolium bromide (MTT) assay was used to determine cell death. HaCaT human keratinocyte and RAW 264.7 macrophage cells were cultured in DMEM supplemented with fetal bovine serum (10%), penicillin (100 U/mL), and streptomycin (100 μg/mL) at 37 °C in 5% CO_2. The cells were seeded into 96-well plates at a cell density of 1×10^4 cells/well for 24 h and then treated with various concentrations of sample solution, followed by a 24 h incubation. MTT solution (5 mg/mL in culture medium) was added, followed by a 3 h incubation. The resulting formazan crystals were solubilized with DMSO (200 μL), and the absorbance was read at 540 nm using a microplate reader (Varioskan LUX multimode microplate reader, Thermo Scientific). The percent inhibition was calculated, and the IC_{50} values were subsequently determined.

$$\text{inhibition(\%)} = \frac{(\text{absorbance control} - \text{absorbance sample})}{\text{absorbance control}} \times 100$$

Determination of Filaggrin and Involucrin by Western Blot. The nontoxic concentrations of nanoemulsion on HaCaT were tested to determine the effect of active nanoemulsions on filaggrin and involucrin levels and investigate promising activity for improving the skin barrier. Anti-involucrin (SY5, Invitrogen) and anti-filaggrin (FLG/1945, Abcam) were used in this experiment. The HaCaT cells were seeded on the 6-well plate (3.0×10^5 cells/well). After 24 h of incubation, the cells were treated with the nanoemulsion samples (0.25−1 μg/mL) for 24 h. The treated cells were further collected after washing with PBS at pH 7.4. Following that, cells were extracted using a RIPA lysis buffer supplemented with protease inhibitors. To obtain the protein lysate, centrifugation was done for 10 min at 3500 rpm. The protein was quantified by Barford assays, with BSA as a standard. The proteins (30 μg/lane) were separated by 12.5% sodium dodecyl sulfate poly(acrylamide gel) electrophoresis (SDS-PAGE). Then, the proteins were transferred onto 0.2 μm poly(vinylidene difluoride) (PVDF) membranes. The Western blot was done for 1 h with 100 V. After blocking in 3% BSA (in 1× TBS-T), the membranes were incubated with primary antibodies (anti-involucrin (1:2000) and anti-filaggrin (1:500)) and then incubated with horseradish peroxidase-conjugated anti-IgG secondary antibody (1:5000) in 5% skim milk (in 1× TBS-T). A GADPH (D4C6R, Cell Signaling Tech, MW = 37 kDa) was used as an internal standard. Detection was done with SuperSignal West Femto Maximum Sensitivity Substrate (No. 34095) for 2 min.

Statistical Analysis. Determination of the IC_{50} and significance difference of the average mean for each group was done using a one-way ANOVA with Tukey's test or an unpaired t test with GraphPad Prism v.9.

https://doi.org/10.1021/acsnanoscienceau.4c00053
ACS Nanosci. Au 2025, 5, 37−51

Table 2. Physicochemical Characteristics of Betamethasone Dipropionate-, Essential Oil-, and Hexane Extract-Loaded Nanoemulsions[a]

no.	sample	particle size (nm)	PDI	zeta potential (mV)	pH (at 25 °C)	EE of BD (%)
1.	EO NE	12.43 ± 0.16[b]	0.26 ± 0.01[c]	−3.74 ± 0.22[e]	5.67 ± 0.35[d]	NA
2.	EO BD NE	13.53 ± 0.09[c]	0.12 ± 0.01[a]	−2.47 ± 0.22[b]	5.24 ± 0.03[a]	95.904 ± 0.628[b]
3.	Hex NE	14.62 ± 0.02[d]	0.33 ± 0.004[d]	−4.38 ± 0.13[c]	5.52 ± 0.08[c]	NA
4.	Hex BD NE	12.32 ± 0.06[b]	0.132 ± 0.002[a]	−5.17 ± 0.17[d]	5.29 ± 0.07[b]	97.481 ± 2.18[a]
5.	blank NE	11.11 ± 0.07[a]	0.21 ± 0.01[b]	−1.23 ± 0.19[a]	5.81 ± 0.03[e]	NA

[a]EE = encapsulation efficiency, NA = not applicable, EO NE = *B. rotunda* EO nanoemulsion, EO BD NE = BD nanoemulsion loaded with *B. rotunda* EO, Hex NE = *B. rotunda* hexane extract nanoemulsion, and Hex BD NE = BD nanoemulsion loaded with *B. rotunda* hexane extract. One-way ANOVA with Tukey's and an unpaired *t* test were used to compare the mean between samples, and different letters indicate a significant difference in each measurement (*p*-value < 0.05).

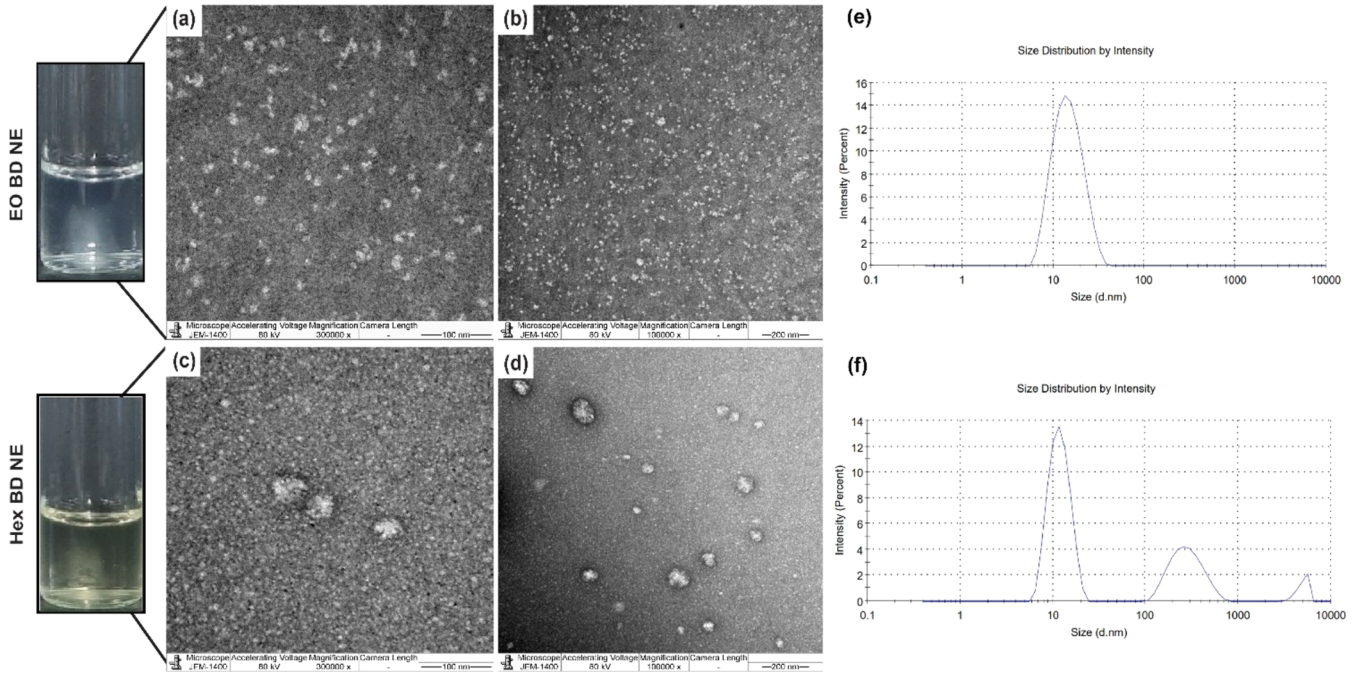

Figure 1. TEM images of negative-stained, BD-loaded nanoemulsions: (a) EO BD NE at 300 000×, (b) EO BD NE at 100 000×, (c) Hex BD NE at 300 000×, and (d) Hex BD NE at 100 000× magnification. Droplet diameters (nm) of BD-loaded nanoemulsions by DLS measurement: (e) EO BD NE and (f) Hex BD NE.

RESULTS AND DISCUSSION

Formulation and Physicochemical Characterization of the Nanoemulsions

In this study, a high-energy ultrasonication method was used to facilitate nanoemulsion formation. The ultrasonication (>20 kHz) created mechanical vibration and acoustic cavitation, breaking up the larger nanoemulsion droplets into smaller droplets.[31] Our finding showed nanoemulsions of *B. rotunda* EO and hexane extract (Hex) loaded with or without BD were successfully prepared by combining spontaneous emulsification and ultrasonication. The composition of the nanoemulsion (NE) is shown in Table 1. The nanoemulsions containing the hexane extract required more sonication time (60 min) and produced slightly larger droplets and PDIs, which may be due to the higher complexity of the phytochemical composition in the hexane extract compared with EO. Extraction with *n*-hexane can yield some low-polar compounds (e.g., flavonoids, carotenoids, and terpenoids).

As shown in Table 2, all of the nanoemulsions had a droplet diameter of less than 20 nm with monodispersity (PDI < 0.7 according to ISO 22,412:2017 standard).[38] Spherical BD nanoemulsions were successfully generated with >95% EE (Figure 1 and Table 2). Our findings revealed a negative zeta potential with a low magnitude generated by nonionic polysorbate-80 as a surfactant. Nanoparticles with a zeta potential value between −10 and +10 mV have a neutral charge.[39] A previous report used oleic acid with a surfactant mixture of Cremophor RH40 and Transcutol P for preparing BD microemulsion, which resulted in 26−192 nm of droplet diameter.[40] Our formulation with olive oil and polysorbate-80 generated smaller droplet sizes. Polysorbate-80 is a nonionic surfactant that has a polar polyoxyethylene head and an oleic acid tail in its structure and a hydrophilic−lipophilic balance value of 15. It is widely used in the food and pharmaceutical industries as an emulsifier. It can stabilize emulsion droplets because of the steric repulsion caused by its large polyoxyethylene head.[41] Consequently, the magnitude of the zeta potential of all of the nanoemulsions was relatively low.

The pH of the nanoemulsions (5.24−5.81) was shown to be suitable for skin applications, which is normally in the range of 4.2−5.6.[42] The pH of the skin is physiologically regulated by the acid mantle, lipid barrier, and epidermal layer. Because of the skin barrier defect, normal skin pH can be altered. *S.*

https://doi.org/10.1021/acsnanoscienceau.4c00053
ACS Nanosci. Au 2025, 5, 37−51

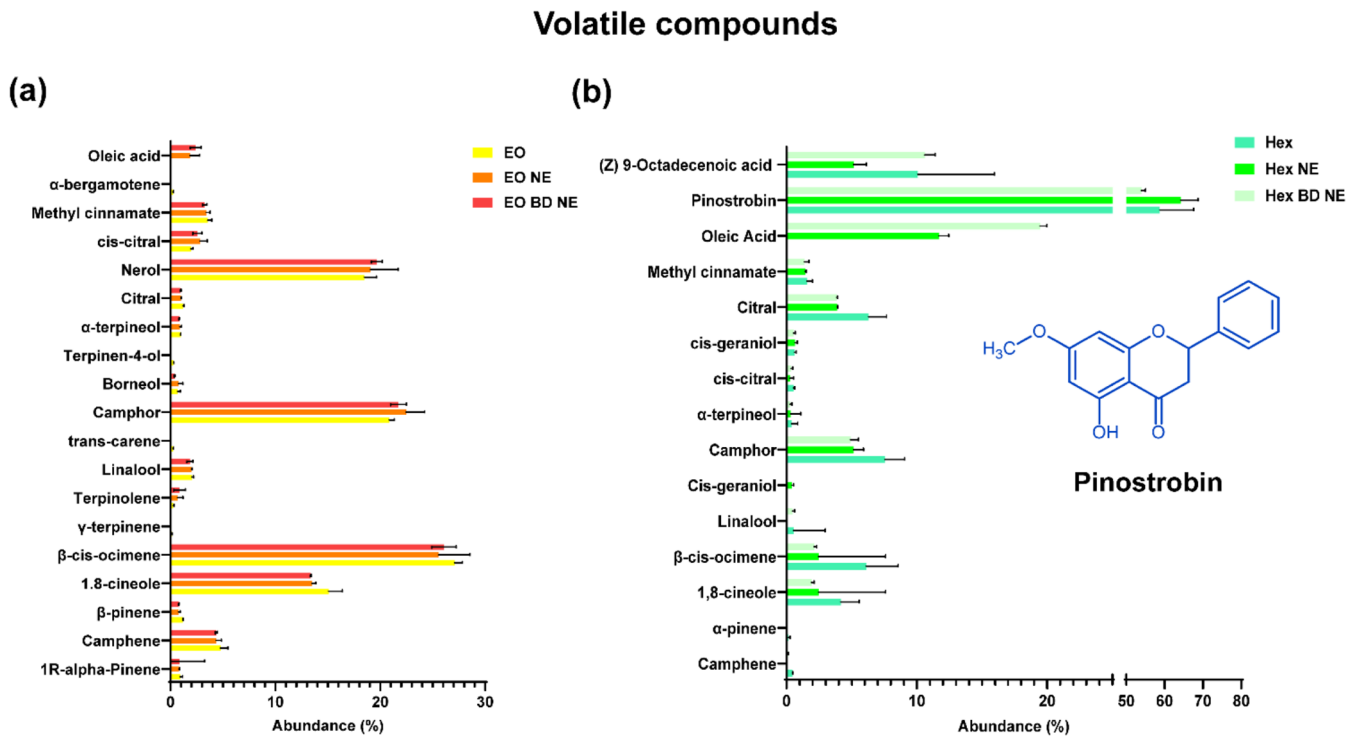

Figure 2. (a) Presence and abundance (%) of volatile phytocompounds found in EO and its nanoemulsions and (b) Hex and its nanoemulsions detected by GC-MS analysis.

aureus, which is known to worsen the severity of AD, exhibits optimal growth at pH values of 7.0−7.5. Therefore, skin care products for AD are recommended to have an acidic pH or pH balance with the normal skin pH (4.5−6.5) to provide a protective effect. A higher pH skin care product may disrupt skin barrier function. To maintain the barrier function of the skin, it is recommended to use products with a pH value of less than 5.5.[42,43]

Chemical characterizations, such as EE measurements and GC−MS, were performed to evaluate the BD content and the composition of volatile phytocomponents in NE. The formulation of BD into the NE with the EO and hexane extract of *B. rotunda* resulted in a high percentage of EE (>95%) and the volatile phytocompounds present in the EO remained during formulation. The loading of phytochemicals into the nanoemulsion was influenced by the solubility of each phytochemical ingredient in the carrier oil use (olive oils), which is primarily composed of oleic acid. Based on the result (Figure 2 and Supporting information, Figure S2, Tables S1 and S2), the composition of the major compounds (β-cis ocimene, camphor, nerol, camphene, and methyl cinnamate) remained the same after formulation, whereas the 1.8-cineole showed a slight decrease after formulation. Moreover, there was an alteration of volatile component compositions in Hex compared with Hex NE. There was a significant reduction in camphor, β-cis ocimene, and citral after the formulation; however, pinostrobin, 9-octadecenoic acid, methyl cinnamate, and some trace components (e.g., cis-geraniol, α-terpineol) remained in the same composition.

According to GC−MS analysis, the formulation method used for nanoemulsions was successful for maintaining the phytochemicals in the EO and hexane extract. Primary volatile components in both EO and hexane extract were still present after formulation. Only trace components were not detected after formulation (e.g., terpinene γ, trans carene, terpinene-4-ol, and α bergamotene; Figure 2 and Table S1). A high oleic acid content was detected in Hex NE, possibly because of the olive oil used in the formulation. The alteration of volatile components occurred after the formulation of Hex NE. Major volatile components (e.g., camphor, β-cis ocimene, and neral) were decreased with an increase in the content of oleic acid because of the olive oil used in the system. This may be attributed to either chemical degradation throughout the 60 min sonication period or extraction efficiency prior to GC−MS analysis.

Short- and Long-Term Stability Tests of the Nanoemulsions

All generated nanoemulsions passed short-term stability tests, including heating and cooling cycles and centrifugation testing; thus, they were subjected to long-term stability testing. A long-term stability test was conducted by monitoring the percentage of transmittance and the pH of the nanoemulsions at three different temperatures. The pH alteration may indicate chemical reactions occurring in the nanoemulsion system during storage because of the microbial growth, components released due to chemical instability, or byproduct discharge.[44] Our finding showed that all nanoemulsions were unstable at 25 °C storage temperature, particularly after one month of storage, as indicated by notable changes in transmittance and pH. Therefore, storing at −20 and 4 °C could maintain the physical and chemical properties, as represented by transmittance and pH (Figure 3). Even after 3 months of storage at −20 °C, all nanoemulsions had a monodisperse PDI (<0.7), suggesting physical stability. NE was not significantly changed in particle size or %EE after 3 months of storage at −20 °C. Although a significant change in PDI was observed after 3 months of storage, particularly for Hex BD NE, the %EE of EO

https://doi.org/10.1021/acsnanoscienceau.4c00053
ACS Nanosci. Au 2025, 5, 37−51

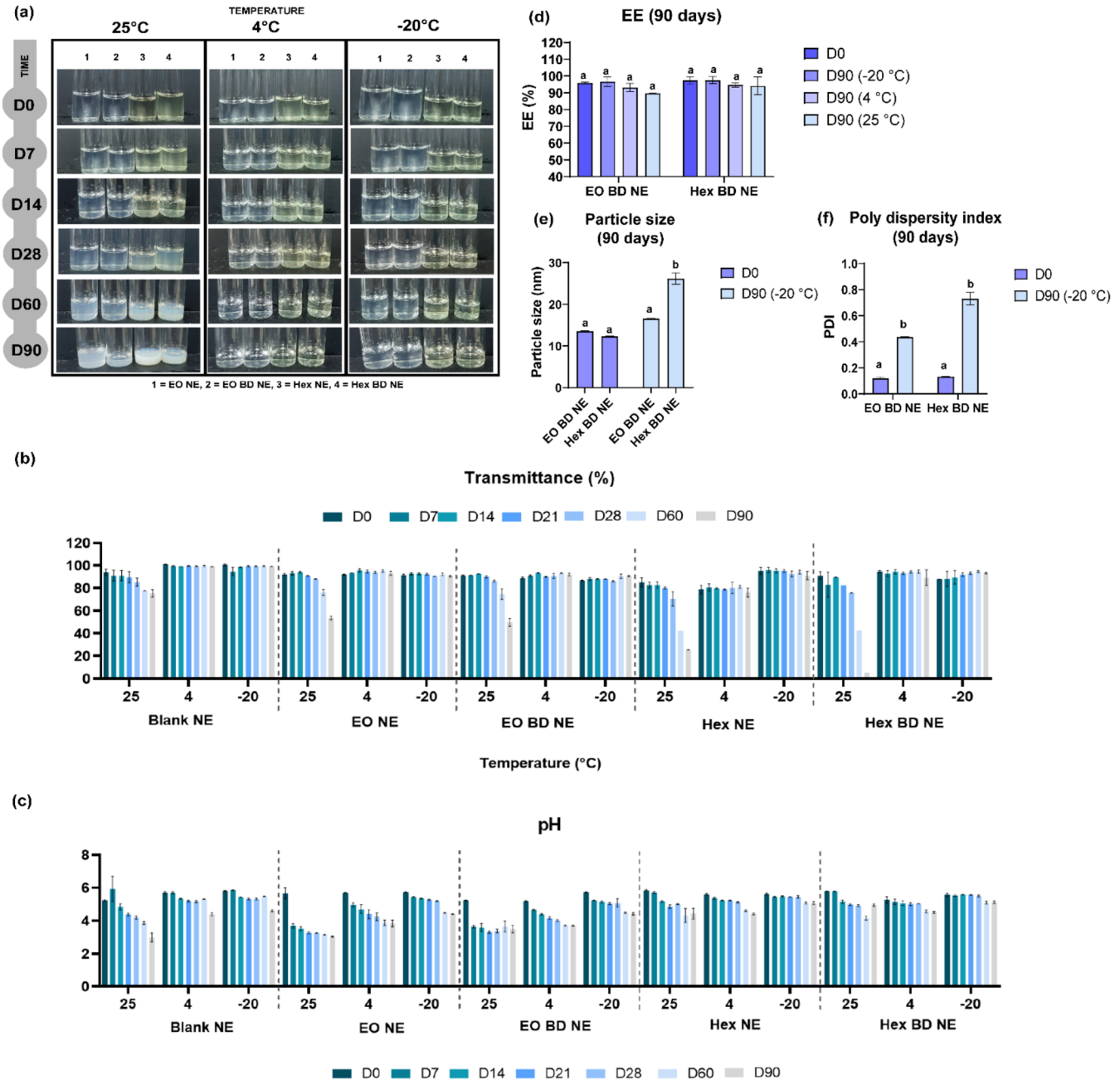

Figure 3. (a) Percent transmittance, (b) pH monitoring during long-term storage (90 days), (c) encapsulation efficiency (%) of EO BD NE and Hex BD NE after 90 days of storage at three different temperatures, (d) particle size, and (e) PDI of EO BD NE and Hex BD NE after 90 days at −20 °C as the optimal storage condition. One-way ANOVA with Tukey's and an unpaired *t* test were used to compare the mean between samples, and different letters indicate a significant difference in each measurement (p-value < 0.05).

BD NE and Hex BD NE were considered stable after 3 months of storage at 4 and −20 °C (Figure 3).

We suggested that the optimal storage condition for maintaining the pH of the generated nanoemulsions was at −20 °C. The decrease in pH of emulsion products prepared with vegetable oils may be caused by fatty acid esters hydrolyzing into free fatty acids.[28] The considerable drop in pH during room temperature storage, as observed for EO NE and EO BD NE, may be caused by this type of hydrolysis.

Antioxidant Activities of the Nanoemulsions

The antioxidative properties of the nanoemulsions were evaluated by using DPPH and NO radical scavenging assays. In addition, the FRAP assay was performed to determine the electron donor ability and ferrous-reducing capacity. *B. rotunda* EO exhibited higher in vitro NO radical inhibitory activity compared with that of the hexane extract. Accordingly, the EO BD NE showed higher NO radical scavenging compared with that of the Hex BD NE (Figure 4 and Table S5).

Based on the NO radical scavenging activity, EO was considered more active than the hexane extract, which also affected the inhibition of NE-containing EO. Our results indicated that EO NE exhibited higher NO radical scavenging activity compared to Hex NE. Conversely, the hexane extract exhibited higher DPPH radical scavenging activity compared with EO. As shown in Figure 4 and Table S5, nanoemulsions containing EO and hexane extract have a 2-fold higher DPPH

https://doi.org/10.1021/acsnanoscienceau.4c00053
ACS Nanosci. Au 2025, 5, 37−51

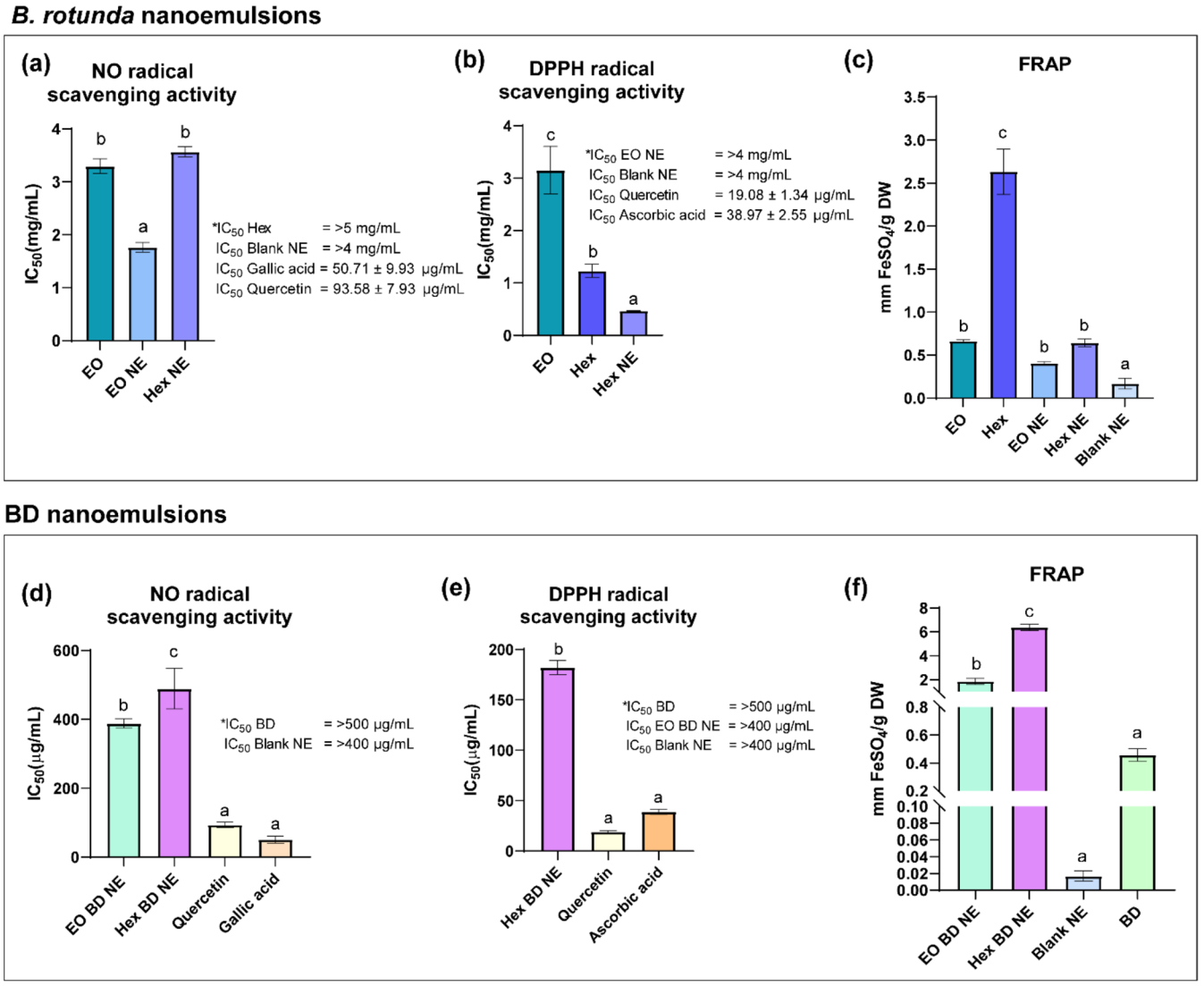

Figure 4. Antioxidant activities of *B. rotunda* essential oils, hexane extract, betamethasone dipropionate, and their nanoemulsions: (a) NO radical scavenging activity of *B. rotunda* nanoemulsions compared to unencapsulated EO/extract, (b) DPPH radical scavenging activity of *B. rotunda* nanoemulsions compared to unencapsulated EO/extract, (c) FRAP activity of *B. rotunda* nanoemulsions compared to unencapsulated EO/extract, (d) NO radical scavenging activity of BD nanoemulsions compared to unencapsulated BD, (e) DPPH radical scavenging activity of BD nanoemulsions compared to unencapsulated BD, and (f) FRAP activity of BD nanoemulsions compared to unencapsulated BD. Extract content in NE was used to compare nanoemulsions loaded with EO/extract and the EO/extract; BD content in NE was used to compare the antioxidant activity between BD and BD nanoemulsions loaded with EO/extract. One-way ANOVA with Tukey's and an unpaired *t* test were used to compare the mean between samples in a sample group, and different letters indicate a significant difference in each experiment (p-value < 0.05).

radical scavenging activity compared with their free-form extracts. The different antioxidant activities of EO NE and Hex NE can be attributed to their unique phytochemical compositions and the resulting solubility and reaction kinetics in aqueous media. As presented in our study, the EO NE primarily consists of oxygenated monoterpenes, which tend to have higher water solubility compared to the nonoxygenated components found predominantly in Hex NE. This higher water solubility of EO components allows them to interact more efficiently with reactive nitrogen species, such as NO radicals, in aqueous environments. Consequently, EO NE demonstrated higher NO radical scavenging activity due to the faster reaction rates of these soluble monoterpenes.

In contrast, Hex NE, which is rich in nonpolar compounds like pinostrobin, exhibited superior DPPH radical scavenging activity. The effectiveness of Hex NE in DPPH assays can be attributed to the synergistic effects of several active compounds, including camphor, 1,8-cineole, linalool, and geranial.[45] These compounds are known to act as electron donors, neutralizing DPPH radicals through mechanisms enhanced by their combined presence in the nanoemulsion. Such interactions suggest that the various components in Hex NE work together to provide a stronger antioxidant effect against the DPPH radicals. Further studies are recommended to isolate and assess the individual radical scavenging activities of the EO and Hex components to further confirm these observations.

Overall, the nanoemulsion formulation showed improvement in NO and DPPH radical scavenging activity; however, the FRAP value decreased significantly after nanoemulsion formulation (p-value < 0.05). The lower ferric-reducing activity of EO or hexane extract nanoemulsion is likely due to the

https://doi.org/10.1021/acsnanoscienceau.4c00053
ACS Nanosci. Au 2025, 5, 37−51

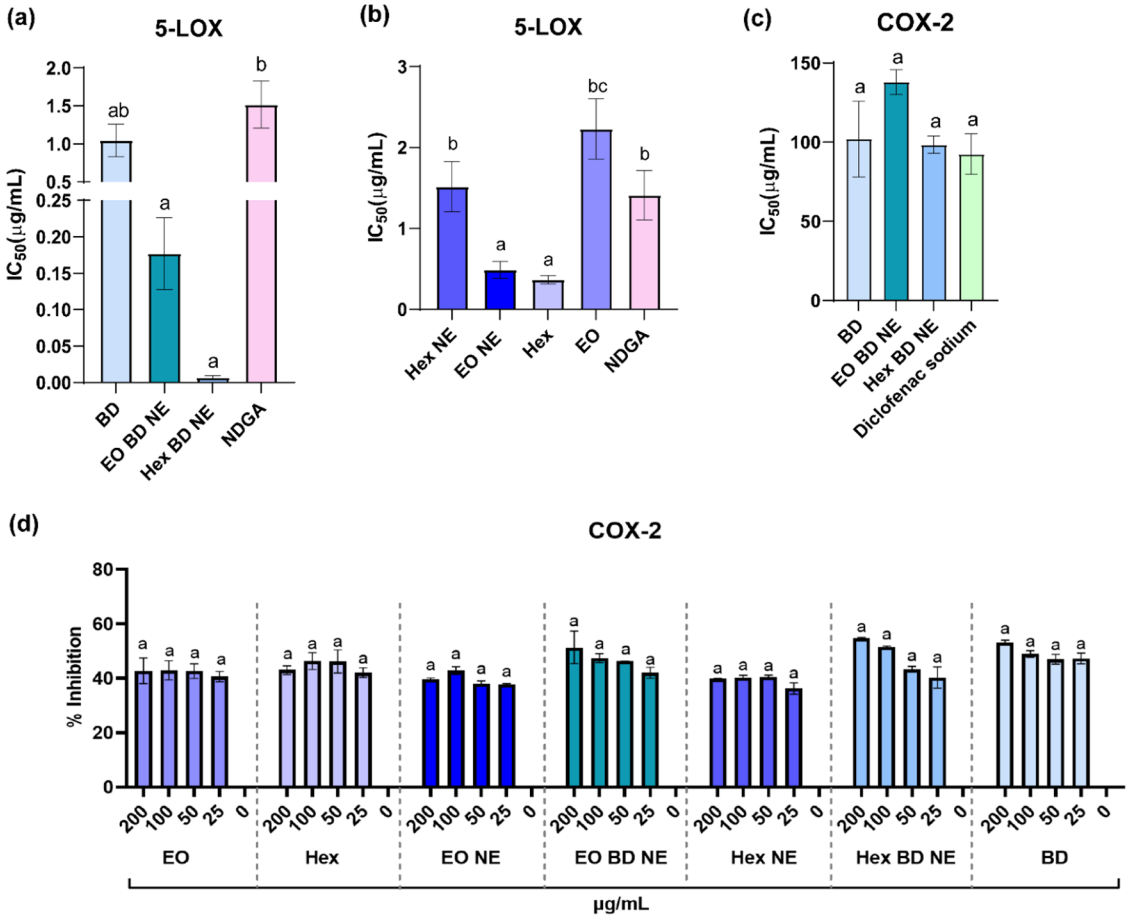

Figure 5. (a) 5-LOX inhibitory activity of the BD nanoemulsion loaded with *B. rotunda* EO and hexane extract, (b) 5-LOX inhibitory activity of *B. rotunda* EO and hexane extract and their nanoemulsion, (c) COX-2 inhibitory activity of the BD nanoemulsion loaded with *B. rotunda* EO and hexane extract, and (d) COX-2 inhibitory activity of *B. rotunda* EO and hexane extract and their nanoemulsion. One-way ANOVA with Tukey's test was used to compare the mean between samples, and different letters indicate a significant difference in each measurement (p-value < 0.05).

prolonged time required for component release from the nanoemulsion. Furthermore, the nanoemulsion formulation of BD with the EO and hexane extract of *B. rotunda* enhanced the antioxidant activity against DPPH and NO. The FRAP values of the BD-loaded nanoemulsions were higher compared with those of BD (Figure 4 and Table S5). The enhancement of radical scavenging activity may result from the improved solubility of lipophilic compounds following nanoemulsion formulation.[46]

Hyperinflammation in AD may occur through oxidative stress caused by *S. aureus* colonization. Thus, our goal is to develop a multiaction nanoformulation for managing AD that includes antioxidant, antibacterial, and anti-inflammatory activities. The nanoemulsion formulation was shown to improve the antioxidant activities, which may be associated with an improvement in solubility. BD displayed low inhibitory activity toward NO and DPPH radicals because of the lack of a hydroxyl moiety in its structure, which resulted in a lower ability to transfer electrons or hydrogen atoms for radical neutralization. The formulation of BD into nanoemulsions containing *B. rotunda* EO and hexane extract markedly enhanced the antioxidant activity against NO and DPPH radicals. In addition, supplementation of the hexane extract with BD nanoemulsions improved the FRAP value 10-fold (Figure 4). The antioxidant capabilities of EO are attributed to the presence of phenol-like compounds, which thrive as free radical scavengers.[47] Several components in *B. rotunda* EO and hexane extract, such as camphor, 1.8-cineole, linalool, β-pinene, and γ-terpinene, have been reported to exhibit ferric-reducing activity and DPPH radical scavenging.[48] These compounds may work synergistically to enhance the antioxidant activity of nanoemulsions containing *B. rotunda* EO or hexane extract. Furthermore, the high phenolic content found in the hexane extract of *B. rotunda*[11] contributes to the antioxidant activity of the nanoemulsions. Since the antioxidant compounds exhibit a protective function against infection and can block proinflammatory mediators during the inflammation process by neutralizing free radicals,[49] the antioxidative properties of our nanoemulsion may act synergistically to suppress the inflammation process.

In Vitro Anti-Inflammatory Effects of the Nanoemulsions

In this study, two main human inflammatory enzymes involved in the arachidonic acid pathway, 5-LOX and COX-2, were targeted to assess the potency of nanoemulsions in suppressing the proinflammatory mediators involved in AD pathogenesis. As shown in Figure 5, the EO NE exhibited 4.5-fold higher 5-LOX inhibitory activity compared with its essential oils, whereas the 5-LOX inhibitory activity of Hex NE was lower compared with that of its free form; however, it was 2-fold higher than NDGA. However, the formulation of nanoemulsions containing BD-loaded essential oils and BD-loaded hexane extract enhanced BD inhibitory activity against 5-LOX

https://doi.org/10.1021/acsnanoscienceau.4c00053
ACS Nanosci. Au 2025, 5, 37−51

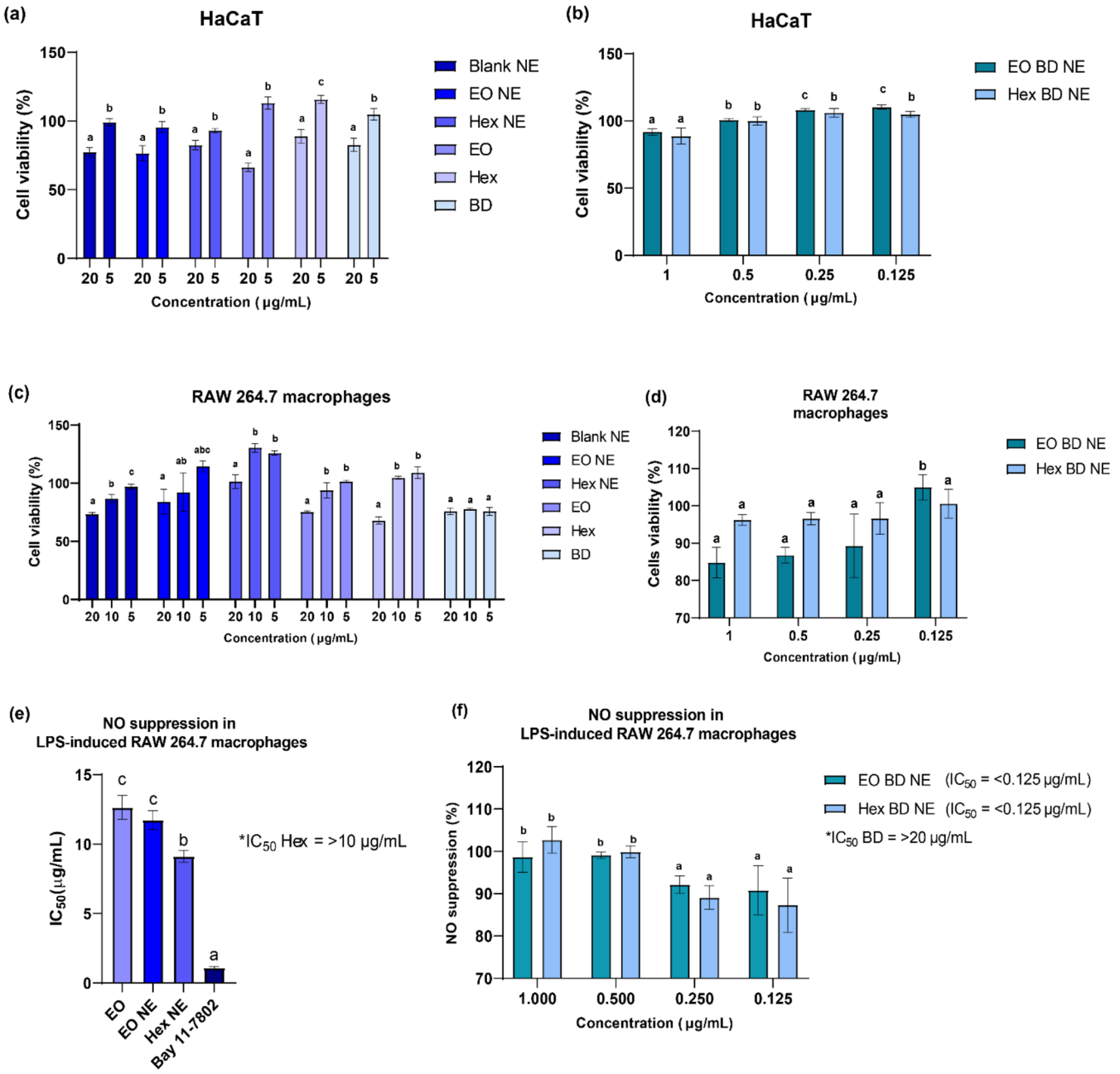

Figure 6. (a) Cell viability of HaCaT cells after treatment with *B. rotunda* EO and hexane extract and their nanoemulsions, (b) cell viability of HaCaT cells after BD nanoemulsion treatment, (c) cell viability of RAW 264.7 macrophage cells after treatment with *B. rotunda* EO and hexane extract and their nanoemulsions, (d) cell viability of RAW 264.7 macrophage cells after BD nanoemulsion treatment, (e) NO suppression (%) in LPS-induced RAW 264.7 macrophages after treatment with *B. rotunda* EO and hexane extract and their nanoemulsions, and (f) NO suppression (%) in LPS-induced RAW 264.7 macrophages after BD nanoemulsion treatment. Hex was toxic to RAW 264.7 macrophages at 20 μg/mL; BD content in NE was used to compare the anti-inflammatory activity between BD and BD nanoemulsion loaded with EO/extract; and a one-way ANOVA with Tukey's test was used to determine significant differences in each group of treatment (p-value < 0.05).

11-fold higher for EO BD NE and 288-fold more for Hex BD NE.

According to the COX-2 inhibition assay, however, it appears that the nanoemulsion formulation of EO and hexane extract did not improve the inhibitory activity. Hex NE exhibited lower COX-2 inhibitory activity compared with its extract, and the same was observed for EO NE. In contrast, the formulation of BD into nanoemulsions loaded with hexane extract slightly improved the COX-2 inhibition activity (Figure 5c), which was comparable with that of the standard NSAID diclofenac sodium. However, the nanoemulsion formulation of BD loaded with EO did not improve COX-2 inhibitory activity. This may be due to the release timing of the active compounds in nanoemulsions. In addition, the low water solubility of phytochemicals in the hexane extract, compared with EO in buffer media, could have influenced the result, as a similar finding was observed with in vitro NO radical inhibition (Figure 4). Additionally, since the free-form extract and EO showed higher activity against 5-LOX compared to COX-2, the nanoemulsion formulation showed a similar trend.

As mentioned above, our formulations of BD with EO and hexane extract successfully enhanced the 5-LOX inhibitory

https://doi.org/10.1021/acsnanoscienceau.4c00053
ACS Nanosci. Au 2025, 5, 37−51

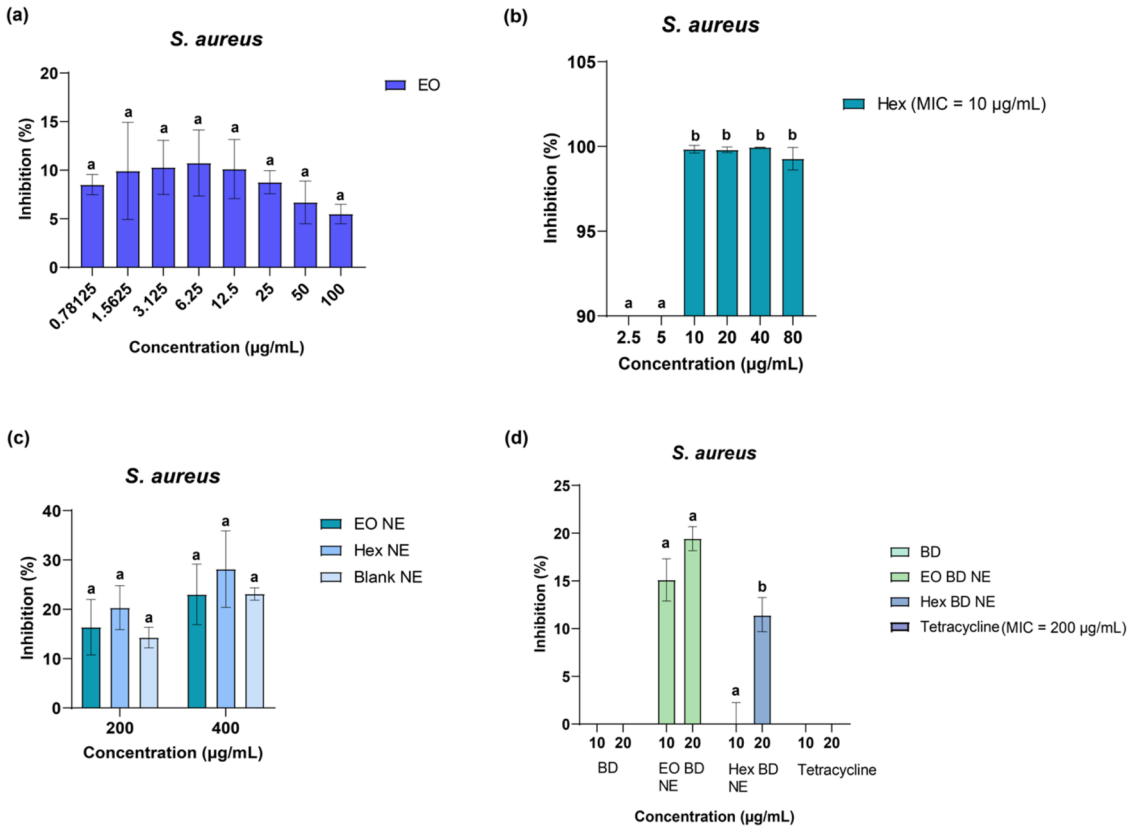

Figure 7. Antibacterial activity determined by the turbidimetric method: (a) *B. rotunda* EO, (b) *B. rotunda* hexane extract, (c) *B. rotunda* EO and hexane extract nanoemulsions, and (d) BD nanoemulsions loaded with EO and hexane extract were compared with BD and antibiotic tetracycline. The BD content in NE was used to compare the antibacterial activity between BD and BD nanoemulsions loaded with EO/extract. One-way ANOVA with Tukey's and an unpaired *t* test was used to compare the mean between samples, and different letters indicate a significant difference in each measurement (p-value < 0.05).

effect. Furthermore, a marked improvement in 5-LOX inhibition was observed in the formula of BD with the hexane extract (p-value < 0.05), which demonstrates the synergistic effect of BD with the hexane extract of *B. rotunda*. The synergistic interaction may be attributed to pinostrobin content, as our previous studies showed that pinostrobin is the primary compound present in hexane extract and exhibited significant 5-LOX activity compared with the standard NSAID NDGA.[50] Further studies are required to clarify the mechanism.

Cytotoxicity of the Nanoemulsions against HaCaT Human Keratinocytes Cells and Suppression of NO Production in LPS-Induced RAW 264.7 Macrophages

The cytotoxicity of *B. rotunda*, BD, and their nanoemulsions was determined by the MTT assay. Our finding demonstrated that *B. rotunda* EO, hexane extract, and their nanoemulsions were nontoxic to HaCaT cells at 5 μg/mL, while the BD nanoemulsions were also nontoxic at 1 μg/mL.

We further tested NO release suppression in LPS-induced RAW 264.7 macrophage cells to assess their anti-inflammatory activity using the same range of nontoxic concentrations. Based on these results, the formulation of EO and hexane extract into NE slightly improved the inhibition of NO production and reduced toxicity in RAW 264.7 macrophage cells (Figure 6). EO, EO NE, and Hex NE exhibited superior NO suppression activity compared to BD as the standard AD treatment. Cytotoxicity against RAW 264.7 cells was also reduced.

Compared with BD, all nanoemulsions were less toxic to RAW 264.7 cells. In addition, the formulation of BD in the *B. rotunda* EO and hexane extract nanoemulsions significantly enhanced NO inhibition in LPS-induced RAW 264.7 macrophages (p-value < 0.05). EO BD NE and Hex BD NE markedly suppressed NO release in LPS-induced RAW 264.7 macrophage cells without toxicity (Figure 6). At concentrations of 0.125 μg/mL, EO BD NE and Hex BD NE suppressed NO production by 90.8 ± 5.8 and 87.3 ± 6.4 μg/mL, respectively. Both BD-loaded nanoemulsions exhibited superior activity compared with standard Bay 11−7802 (Figure 6).

The BD nanoemulsion loaded with the hexane extract demonstrated its significant activity in suppressing NO release in RAW 264.7 macrophage cells while being notably nontoxic to both RAW 264.7 macrophages and HaCaT keratinocyte cells. Pinostrobin, a major bioactive compound in the hexane extract detected by GC-MS, may play a role in suppressing the NO production in RAW 264.7 macrophage cells. Pinostrobin suppresses NO production as well as iNOS and COX-2 expression in LPS-induced RAW 264.7 macrophage cells.[51] Other phytochemicals present in the hexane extract may influence the NO suppression activity. Various components present in EO and Hex have been reported to reduce NO production, such as α-pinene (in RAW 264.7 macrophages cells),[52] 1.8-cineole/eucalyptol (in LPS-induced HUVECs human umbilical vein endothelial cells),[53] and oleic acid (in LPS stimulated BV2 murine microglia cells).[54] Consequently, these components may also contribute to the enhancement of

https://doi.org/10.1021/acsnanoscienceau.4c00053
ACS Nanosci. Au 2025, 5, 37−51

the NO-suppressing activity of nanoemulsions containing *B. rotunda* EO and hexane extract. NO is involved in recurrent chronic inflammation in AD; a higher level of NO was found in AD skin compared to the normal one.[19] By suppressing NO release, our formula showed promise to reduce inflammation and may be beneficial for reducing inflammation in AD skin.

Antibacterial Activity of the Nanoemulsions

Since AD skin is characterized by *S. aureus* colonization, we assessed the antibacterial activity of BD, EO, hexane extract, and their nanoemulsions. The hexane extract showed superior antibacterial activity compared to the antibiotic tetracycline, with MIC values of 10 and 200 μg/mL, respectively. Nanoemulsion formulations prepared with *B. rotunda* EO slightly improved *S. aureus* inhibitory activity. Meanwhile, the nanoemulsions of the hexane extract were less active compared to the free form (Figure 7). This phenomenon may be influenced by the time release of the active compounds in NE. In contrast, the *S. aureus* inhibitory activity of BD was significantly improved (p-value < 0.05) in its nanoemulsion form (Figure 7). At concentrations up to 20 μg/mL, BD nanoemulsions loaded with EO or hexane extract exhibited stronger activity compared to tetracycline (Figure 7d). The NE form of BD loaded with the hexane extract showed promising antibacterial activity against *S. aureus*.

The small size of the nanoemulsion increases its surface area, leading to more effective interaction with bacterial cell membranes. Additionally, the improved solubility of lipophilic components, such as EO, hexane extract, and BD, enhances dispersion, leading to better cell contact. The lipophilic surface of nanoemulsion droplets facilitates membrane permeability, allowing integration with bacterial cell membranes. This interaction disrupts the membrane, ultimately causing cell death.[46]

In Vitro Skin Barrier Repair Effects of the Nanoemulsions

Involucrin and filaggrin, as epidermal barrier protein markers, were investigated to assess the activity of selected nanoemulsions for skin barrier repair. EO BD NE and Hex BD NE were further tested as they significantly enhanced NO release suppression in LPS-induced RAW 264.7 macrophages without any toxic effect on human keratinocyte HaCaT cells.

Filaggrin expression was shown to increase following treatment with BD, EO BD NE, and Hex BD NE. The results demonstrated that involucrin and filaggrin expression increased after treatment with Hex BD NE at 0.25 and 1 μg/mL (Figure 8). Compared to BD at 1 μg/mL, Hex BD NE (0.25 μg/mL) exhibited a greater ability to stimulate involucrin expression.

The epidermal skin is primarily composed of keratinocytes, which undergo differentiation for skin barrier function. During differentiation, keratinocytes produced various barrier molecules, including filaggrin and involucrin.[22] People with AD showed downregulation of involucrin and filaggrin protein, leading to skin barrier dysfunction.[55] Filaggrin plays an essential role in skin barrier by aggregating the keratin in the epidermis, leading to skin cell compaction.[56] The improvement of the filaggrin level improves barrier function and skin hydration. It may also promote the natural moisturizing factor production that eventually will maintain skin's protective function.[57] On the other hand, involucrin plays a critical role in the formation of the cornified envelope for reinforcing the skin barrier.[24] Involucrin is a structural protein, which is cross-linked in the epidermis, providing integrity of skin. Enhancement of involucrin expression resulted in robust cornified envelope formation. Accordingly, these two proteins were investigated to observe the activity of nanoemulsions as skin barrier repair agents.

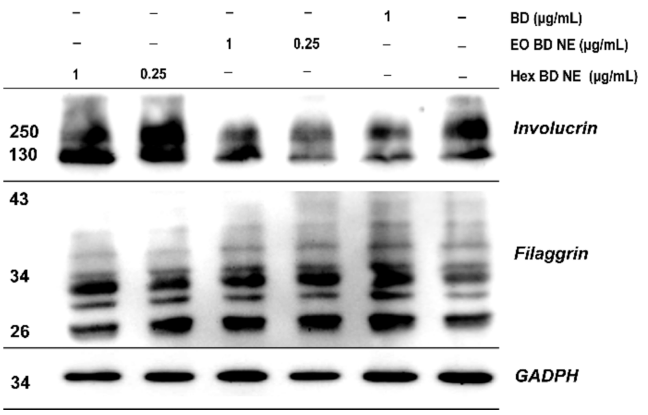

Figure 8. Involucrin and filaggrin expression in HaCaT cells after treatment with EO BD NE (0.25 and 1 μg/mL) and Hex BD NE (0.25 and 1 μg/mL) nanoemulsions compared to BD.

According to the results (Figure 8), the EO BD NE and Hex BD NE were shown to improve the involucrin and filaggrin expression levels as compared with untreated HaCaT cells. Particularly, Hex BD NE (at 0.25−1 μg/mL) showed the ability to induce upregulation of involucrin as compared to the standard AD medication, BD (at 1 μg/mL). It implied that the EO BD NE and Hex BD NE nanoemulsions have promising activity not only to suppress inflammation but also to repair the skin barrier defect in AD. These two promising nanoemulsions may also be applied as preventive agents to restore skin barrier function, thereby preventing the development of AD skin lesions. The involucrin and filaggrin expression may be increased through various possible mechanisms such as the anti-inflammatory effect of the nanoemulsions, which can prevent this protein degradation and promote protein synthesis.

The enhanced upregulation of involucrin expression observed with Hex BD NE treatment compared with EO BD NE and BD alone could be attributed to the specific active components present in the hexane extract. Notably, Hex BD NE contains a relatively high concentration of pinostrobin (53.98%), a lipophilic compound that may play a significant role in promoting upregulation of involucrin expression. While both EO BD NE and Hex BD NE share common essential oil components, the higher composition of pinostrobin in Hex BD NE could contribute to the more pronounced effect observed. Further studies are needed to confirm the specific activity of pinostrobin in enhancing involucrin expression. Additionally, the components used in the nanoemulsion formulation, such as glycerol and free fatty acids derived from olive oil, might also contribute to the upregulation of involucrin and filaggrin expression, as suggested by previous research.[58−60] These findings indicate that a combination of specific lipophilic compounds and the formulation's components may be responsible for the superior performance of Hex BD NE in this context.

In brief, based on in vitro anti-inflammatory enzyme assays (5-LOX and COX-2) and LPS-induced macrophages, the BD formulation loaded with hexane extract achieved the desired anti-inflammatory activity by suppressing 5-LOX, COX-2, and NO, as well as lowering the BD dose loaded without toxic effects on HaCaT human keratinocyte and RAW 264.7

https://doi.org/10.1021/acsnanoscienceau.4c00053
ACS Nanosci. Au 2025, 5, 37−51

macrophage cell lines. Furthermore, supplementation with antioxidants and antibacterial agents against *S. aureus* was also achieved using this formula. Hex BD NE showed high activity against DPPH and NO radicals and a high FRAP value compared with that of EO BD NE. The antibacterial effect of the hexane extract was superior to that of the antibiotic drug tetracycline. The antibacterial activity of the EO and hexane extracts can be attributed to the EO components. The hydrophobicity of EO enables them to be incorporated into bacterial cell membranes.[61] Similarly, free fatty acids consisting of fixed oils have destructive effects on metabolism in the cell membrane, resulting in bacterial death.[62] The oleic acid content of NE compared with that of its free form may attenuate its higher antibacterial activity. The high oleic acid content of NE was from olive oil used as a carrier oil in the nanoemulsion system. Oleic acid is an effective antibacterial agent against *S. aureus* through its disruption of the bacterial cell membrane. These findings suggest the successful formulation of stable nanoemulsions that are compatible with skin pH and exhibit promising anti-inflammatory, antibacterial, and antioxidant activities with no toxic effects on HaCaT human keratinocytes or RAW 264.7 macrophages. Developing BD into nanoemulsions was also associated with reduced cytotoxicity. Furthermore, the EO BD NE and Hex BD NE nanoemulsions showed promising activity as skin barrier repair agents by increasing the levels of involucrin and filaggrin expression. These effects were valuable in skin care formulation in order to improve skin health and integrity as a preventive strategy for AD management. However, further studies are needed to enhance the stability of nanoemulsions at room temperature, investigate the release profile of active components, determine any potential degradation products (e.g., using mass spectroscopy or nuclear magnetic resonance spectroscopy), and evaluate their efficacy in an in vivo AD model.

CONCLUSIONS

AD is a complex skin condition involving inflammation, oxidative stress, skin dryness, and staphylococcal infection. The nanoemulsion formulation of BD containing *B. rotunda* enhanced significant anti-inflammatory properties in terms of 5-LOX inhibition and NO release suppression in LPS-induced RAW 264.7 macrophages while being nontoxic to both HaCaT human keratinocyte and RAW 264.7 macrophage cells. They also have promising properties to restore and maintain the skin barrier. Our formulation may offer a promising multifunctional formula for future topical therapy in suppressing inflammation and skin barrier repair and providing antioxidant and antibacterial activities for AD management. In-cell and in vivo studies using an AD model are recommended for further study of the nanoemulsion efficacy. In addition, further characterization, such as Fourier transform infrared spectroscopy and drug release kinetics, is warranted. Our findings suggest the topical application of *B. rotunda* nanoemulsion and BD-loaded *B. rotunda* nanoemulsion for AD therapy.

ASSOCIATED CONTENT

Supporting Information

The Supporting Information is available free of charge at https://pubs.acs.org/doi/10.1021/acsnanoscienceau.4c00053.

Encapsulation efficiency determination by high−performance liquid chromatography; gas chromatography−mass spectrometry analysis of *Boesenbergia rotunda* essential oils and hexane extract, and their nanoemulsions; long-term stability test by percentage of transmittance monitoring; long-term stability test by pH monitoring; antioxidant activities of *B. rotunda* essential oils, hexane extract, betamethasone dipropionate, and nanoemulsions; DPPH radical scavenging activity of betamethasone dipropionate (BD); nitric oxide (NO) radical scavenging activity of betamethasone dipropionate; anti-inflammatory activities of *B. rotunda* EO, hexane extract, and their nanoemulsions against 5-lipoxygenase (5-LOX) and cyclooxygenase-2 (COX-2); anti-inflammatory activities of betamethasone dipropionate and its nanoemulsions against 5-lipoxygenase (5-LOX) and cyclooxygenase-2 (COX-2) (PDF)

AUTHOR INFORMATION

Corresponding Author

Anuchit Phanumartwiwath − *College of Public Health Sciences, Chulalongkorn University, Bangkok 10330, Thailand;* orcid.org/0000-0001-8731-3875; Email: anuchit.p@chula.ac.th

Authors

Desy Liana − *College of Public Health Sciences, Chulalongkorn University, Bangkok 10330, Thailand*

Jaruwan Chatwichien − *Program in Chemical Sciences, Chulabhorn Graduate Institute, Bangkok 10210, Thailand; Chulabhorn Royal Academy, Bangkok 10210, Thailand*

Complete contact information is available at: https://pubs.acs.org/10.1021/acsnanoscienceau.4c00053

Author Contributions

D.L.: conceptualization, methodology, investigation, data curation, analysis, and writing—original draft preparation. J.C.: investigation, data curation, and writing—review and editing. A.P.: conceptualization, supervision, methodology, analysis, visualization, funding acquisition, and writing—review and editing. All authors have read and agreed to the final version of the manuscript. CRediT: **Desy Liana** conceptualization, data curation, formal analysis, investigation, methodology, writing - original draft; **jaruwan chatwichien** data curation, investigation, writing - review & editing; **Anuchit Phanumartwiwath** conceptualization, formal analysis, funding acquisition, methodology, supervision, visualization, writing - review & editing.

Funding

This study was supported by the 90th Anniversary of Chulalongkorn University Scholarship, Ratchadaphiseksomphot Endowment Fund, Overseas Research Experience Scholarship Fiscal Year 2024, and the Grants for Development of New Faculty Staff, Ratchadaphiseksomphot Endowment Fund, Chulalongkorn University (DNS 66_004_53_002_3).

Notes

The authors declare no competing financial interest.

ACKNOWLEDGMENTS

The authors would like to express their sincere gratitude to Associate Professor Chanida Palanuvej, Somchai Issaravanich, and Maneewan Suwatronnakor for GC−MS instrumental assistance at the College of Public Health Sciences,

Chulalongkorn University. In addition, the authors thank Associate Professor Rojana Sukchawalit and Benya Nontaleerak at Chulabhorn Research Institute for antibacterial assistance. The graphic illustration was partly created using BioRender (BioRender, https://biorender.com/).

REFERENCES

(1) Devillers, A. C. A.; Oranje, A. P. Efficacy and safety of 'wet-wrap' dressings as an intervention treatment in children with severe and/or refractory atopic dermatitis: a critical review of the literature. *Br. J. Dermatol.* **2006**, *154*, 579−585.
(2) Zulfakar, M. H.; Abdelouahab, N.; Heard, C. M. Enhanced topical delivery and ex vivo anti-inflammatory activity from a betamethasone dipropionate formulation containing fish oil. *Inflamm Res.* **2010**, *59*, 23−30.
(3) Alam, M. S.; Ali, M. S.; Alam, N.; Alam, M. I.; Anwer, T.; Imam, F.; Ali, M. D.; Siddiqui, M. R.; Shamim, M. Design and characterization of nanostructure topical gel of betamethasone dipropionate for psoriasis. *J. Appl. Pharm. Sci.* **2012**, *2* (10), 148−158.
(4) Hanna, P. A.; Ghorab, M. M.; Gad, S. Development of Betamethasone Dipropionate-Loaded Nanostructured Lipid Carriers for Topical and Transdermal Delivery. *Anti-Inflammatory Anti-Allergy Agents Med. Chem.* **2019**, *18*, 26−44.
(5) Coondoo, A.; Phiske, M.; Verma, S.; Lahiri, K. Side-effects of topical steroids: A long overdue revisit. *Indian Dermatol. Online J.* **2014**, *5*, 416−425.
(6) Daniel, B. S.; Orchard, D. Ocular side−effects of topical corticosteroids: what a dermatologist needs to know. *Aust. J. Dermatol.* **2015**, *56*, 164−169.
(7) Lim, T. K.; Lim, T. K. Boesenbergia rotunda. In *Edible Medicinal and Non-Medicinal Plants: Vol. 12 Modified Stems, Roots, Bulbs*; Springer International Publishing: Cham, 2016; pp 214−232.
(8) Eng-Chong, T.; Yean-Kee, L.; Chin-Fei, C.; Choon-Han, H.; Sher-Ming, W.; Li-Ping, C. T.; Gen-Teck, F.; Khalid, N.; Abd Rahman, N.; Karsani, S. A.; et al. Boesenbergia rotunda: From Ethnomedicine to Drug Discovery. *Evidence-Based Complementary Altern. Med.* **2012**, *2012*, No. 473637.
(9) Rosdianto, A. M.; Puspitasari, I. M.; Lesmana, R.; Levita, J. Inhibitory Activity of *Boesenbergia rotunda* (L.) Mansf. Rhizome towards the Expression of Akt and NF-KappaB p65 in Acetic Acid-Induced Wistar Rats. *Evidence-Based Complementary Altern. Med.* **2020**, *2020*, No. 6940313.
(10) Kim, M.-S.; Pyun, H.-B.; Hwang, J.-K. Effects of orally administered fingerroot (Boesenbergia pandurata) extract on oxazolone-induced atopic dermatitis-like skin lesions in hairless mice. *Food Sci. Biotechnol.* **2013**, *22*, 257−264.
(11) Liana, D.; Eurtivong, C.; Phanumartwiwath, A. Boesenbergia rotunda and Its Pinostrobin for Atopic Dermatitis: Dual 5-Lipoxygenase and Cyclooxygenase-2 Inhibitor and Its Mechanistic Study through Steady-State Kinetics and Molecular Modeling. *Antioxidants* **2024**, *13*, 74.
(12) Andoh, T.; Haza, S.; Saito, A.; Kuraishi, Y. Involvement of leukotriene B4 in spontaneous itch-related behaviour in NC mice with atopic dermatitis-like skin lesions. *Exp. Dermatol.* **2011**, *20*, 894−898.
(13) Chari, S.; Clark-Loeser, L.; Shupack, J.; Washenik, K. A Role for Leukotriene Antagonists in Atopic Dermatitis? *Am. J. Clin. Dermatol.* **2001**, *2*, 1−6.
(14) Tang, L.; Li, X.-L.; Deng, Z.-X.; Xiao, Y.; Cheng, Y.-H.; Li, J.; Ding, H. Conjugated linoleic acid attenuates 2, 4-dinitrofluorobenzene-induced atopic dermatitis in mice through dual inhibition of COX-2/5-LOX and TLR4/NF-κB signaling. *J. Nutr. Biochem.* **2020**, *81*, No. 108379.
(15) Carola, C.; Salazar, A.; Rakers, C.; Himbert, F.; Do, Q. T.; Bernard, P.; von Hagen, J. A Cornflower Extract Containing N-Feruloylserotonin Reduces Inflammation in Human Skin by Neutralizing CCL17 and CCL22 and Inhibiting COX-2 and 5-LOX. *Mediators Inflammation* **2021**, *2021*, No. 6652791.
(16) Fleischer, A.; Cincinnati, O.; Nam, K.; Kim, J.; Ahn, K.; Hwankyu; Kang, H.; Choi, J.; Choi, B. J.; Lee, S.; et al. Q301 (Zileuton) cream demonstrates superiority to vehicle in improving atopic dermatitis: Results from a phase 2A trial. *JAAD* **2019**, *81*, AB112.
(17) Kim, D.-H.; Ho-Sueb, S. Atopic Dermatitis-Related Inflammation in Macrophages and Keratinocytes: The Inhibitory Effects of Bee Venom. *J. Acupunct. Res.* **2019**, *36*, 80−87.
(18) Lee, D.-h.; Park, J.-k.; Choi, J.; Jang, H.; Seol, J.-w. Anti-inflammatory effects of natural flavonoid diosmetin in IL-4 and LPS-induced macrophage activation and atopic dermatitis model. *Int. Immunopharmacol.* **2020**, *89*, No. 107046.
(19) Akdeniz, N.; Aktaş, A.; Erdem, T.; Akyüz, M.; Özdemir, Ş. Nitric oxide levels in atopic dermatitis. *Pain Clinic* **2004**, *16*, 401−405.
(20) Alessandrello, C.; Sanfilippo, S.; Minciullo, P. L.; Gangemi, S. An Overview on Atopic Dermatitis, Oxidative Stress, and Psychological Stress: Possible Role of Nutraceuticals as an Additional Therapeutic Strategy. *Int. J. Mol. Sci.* **2024**, *25*, 5020.
(21) Morita, H.; Semma, M.; Hori, M.; Kitano, Y. Clinical Application of Nitric Oxide Synthase Inhibitor for Atopic Dermatitis. *Int. J. Dermatol.* **1995**, *34*, 294−295.
(22) Furue, M. Regulation of Filaggrin, Loricrin, and Involucrin by IL-4, IL-13, IL-17A, IL-22, AHR, and NRF2: Pathogenic Implications in Atopic Dermatitis. *Int. J. Mol. Sci.* **2020**, *21*, 5382 DOI: 10.3390/ijms21155382.
(23) Zaniboni, M. C.; Samorano, L. P.; Orfali, R. L.; Aoki, V. Skin barrier in atopic dermatitis: beyond filaggrin. *An. Bras. Dermatol.* **2016**, *91*, 472−478.
(24) Proksch, E.; Fölster-Holst, R.; Jensen, J.-M. Skin barrier function, epidermal proliferation and differentiation in eczema. *J. Dermatol. Sci.* **2006**, *43*, 159−169.
(25) Da Costa, S.; Basri, M.; Shamsudin, N.; Basri, H. Formation of Stable Palm Kernel Oil Esters Nanoemulsion System Containing Hydrocortisone. *Asian J. Chem.* **2014**, *26* (10), 2883−2888, DOI: 10.14233/ajchem.2014.15929.
(26) Garcia, C. R.; Malik, M. H.; Biswas, S.; Tam, V. H.; Rumbaugh, K. P.; Li, W.; Liu, X. Nanoemulsion delivery systems for enhanced efficacy of antimicrobials and essential oils. *Biomater. Sci.* **2022**, *10* (3), 633−653, DOI: 10.1039/D1BM01537K.
(27) Preeti; Sambhakar, S.; Malik, R.; Bhatia, S.; Al Harrasi, A.; Rani, C.; Saharan, R.; Kumar, S.; Geeta; Sehrawat, R. Nanoemulsion: An Emerging Novel Technology for Improving the Bioavailability of Drugs. *Scientifica* **2023**, *2023*, No. 6640103.
(28) Bernardi, D. S.; Pereira, T. A.; Maciel, N. R.; Bortoloto, J.; Viera, G. S.; Oliveira, G. C.; Rocha-Filho, P. A. Formation and stability of oil-in-water nanoemulsions containing rice bran oil: in vitro and in vivo assessments. *J. Nanobiotechnol.* **2011**, *9*, 44.
(29) Safaya, M.; Rotliwala, Y. C. Nanoemulsions: A review on low energy formulation methods, characterization, applications and optimization technique. *Mater. Today Proc.* **2020**, *27*, 454−459.
(30) Gharibzahedi, S. M. T.; Jafari, S. M. Chapter 9-Fabrication of Nanoemulsions by Ultrasonication. In *Nanoemulsions*; Jafari, S. M.; McClements, D. J., Eds.; Academic Press, 2018; pp 233−285.
(31) Ghosh, V.; Mukherjee, A.; Chandrasekaran, N. Ultrasonic emulsification of food-grade nanoemulsion formulation and evaluation of its bactericidal activity. *Ultrason. Sonochem.* **2013**, *20*, 338−344.
(32) Tang, S. Y.; Manickam, S.; Wei, T. K.; Nashiru, B. Formulation development and optimization of a novel Cremophore EL-based nanoemulsion using ultrasound cavitation. *Ultrason. Sonochem.* **2012**, *19*, 330−345.
(33) Yahya, N. A.; Wahab, R. A.; Attan, N.; Hashim, S. E.; Abdul Hamid, M.; Mohamed Noor, N.; Abdul Rahman, A. Optimization of oil-in-water nanoemulsion system of Ananas comosus peels extract by D-optimal mixture design and its physicochemical properties. *J. Dispersion Sci. Technol.* **2020**, 302−315.
(34) Mahran, A.; Ismail, S.; Allam, A. A. Development of Triamcinolone Acetonide-Loaded Microemulsion as a Prospective

Ophthalmic Delivery System for Treatment of Uveitis: In Vitro and In Vivo Evaluation. *Pharmaceutics* **2021**, *13*, 444.
(35) Chew, C. Y.; Chua, L. S.; Soontorngun, N.; Lee, C. T. Discovering potential bioactive compounds from Tualang honey. *Agric. Nat. Resour.* **2018**, *52*, 361−365.
(36) Mogana, R.; Teng-Jin, K.; Wiart, C. The Medicinal Timber Canarium patentinervium Miq. (Burseraceae Kunth.) Is an Anti-Inflammatory Bioresource of Dual Inhibitors of Cyclooxygenase (COX) and 5-Lipoxygenase (5-LOX). *ISRN Biotechnol.* **2013**, *2013*, No. 986361.
(37) Sukandar, E. R.; Kaennakam, S.; Wongsuwan, S.; Chatwichien, J.; Krobthong, S.; Yingchutrakul, Y.; Mahatnirunkul, T.; Mulya, F.; Parasuk, V.; Harding, D. J.; et al. Schomburginones A−J, geranylated benzophenones from the leaves of Garcinia schomburgkiana and their cytotoxic and anti-inflammatory activities. *Phytochemistry* **2023**, *211*, No. 113701.
(38) Sarmah, S.; Gogoi, S. B.; Xianfeng, F.; Baruah, A. A. Characterization and identification of the most appropriate nonionic surfactant for enhanced oil recovery. *J. Pet. Explor. Prod. Technol.* **2020**, *10*, 115−123.
(39) Clogston, J. D.; Patri, A. K. Zeta potential measurement. *Methods Mol. Biol.* **2011**, *697*, 63−70.
(40) Tung, N.-T.; Vu, V.-D.; Nguyen, P.-L. DoE-based development, physicochemical characterization, and pharmacological evaluation of a topical hydrogel containing betamethasone dipropionate micro-emulsion. *Colloids Surf., B* **2019**, *181*, 480−488.
(41) Walia, N.; Zhang, S.; Wismer, W.; Chen, L. A low energy approach to develop nanoemulsion by combining pea protein and Tween 80 and its application for vitamin D delivery. *Food Hydrocolloids Health* **2022**, *2*, No. 100078.
(42) Kuo, S.-H.; Shen, C.-J.; Shen, C.-F.; Cheng, C.-M. Role of pH Value in Clinically Relevant Diagnosis. *Diagnostics* **2020**, *10*, 107.
(43) Schreml, S.; Kemper, M.; Abels, C. Skin pH in the elderly and appropriate skin care. *J. Eur. Med. J. Dermatol.* **2014**, *2*, 86−94.
(44) Denyer, S. P.; Baird, R. M. *Guide to Microbiological Control in Pharmaceuticals and Medical Devices*, 2nd ed.; CRC Press, 2006.
(45) Sharopov, F. S.; Wink, M.; Setzer, W. N. Radical Scavenging and Antioxidant Activities of Essential Oil Components − An Experimental and Computational Investigation. *Nat. Prod. Commun.* **2015**, *10* (1), 1934578X1501000135 DOI: 10.1177/1934578X1501000135.
(46) Manzoor, A.; Asif, M.; Khalid, S. H.; Ullah Khan, I.; Asghar, S. Nanosizing of Lavender, Basil, and Clove Essential Oils into Microemulsions for Enhanced Antioxidant Potential and Antibacterial and Antibiofilm Activities. *ACS Omega* **2023**, *8*, 40600−40612.
(47) Tongnuanchan, P.; Benjakul, S. Essential oils: extraction, bioactivities, and their uses for food preservation. *J. Food Sci.* **2014**, *79*, R1231−R1249.
(48) Sharopov, F. S.; Wink, M.; Setzer, W. N. Radical scavenging and antioxidant activities of essential oil components–an experimental and computational investigation. *Nat. Prod. Commun.* **2015**, *10* (1), 1934578X1501000135.
(49) Brambilla, D.; Mancuso, C.; Scuderi, M. R.; Bosco, P.; Cantarella, G.; Lempereur, L.; Di Benedetto, G.; Pezzino, S.; Bernardini, R. The role of antioxidant supplement in immune system, neoplastic, and neurodegenerative disorders: a point of view for an assessment of the risk/benefit profile. *Nutr J.* **2008**, *7*, 29.
(50) Song, J.-K.; Du, L.-D.; Qiang, G.-F.; Du, G.-H. Camphor. In *Natural Small Molecule Drugs from Plants*; Du, G.-H., Ed.; Springer Singapore: Singapore, 2018; pp 205−208.
(51) Athapaththu, A. M. G. K.; Lee, K. T.; Kavinda, M. H. D.; Lee, S.; Kang, S.; Lee, M.-H.; Kang, C.-H.; Choi, Y. H.; Kim, G.-Y. Pinostrobin ameliorates lipopolysaccharide (LPS)-induced inflammation and endotoxemia by inhibiting LPS binding to the TLR4/MD2 complex. *Biomed. Pharmacother.* **2022**, *156*, No. 113874.
(52) Lin, W.-T.; He, Y.-H.; Lo, Y.-H.; Chiang, Y.-T.; Wang, S.-Y.; Bezirganoglu, I.; Kumar, K. J. S. Essential Oil from Glossogyne tenuifolia Inhibits Lipopolysaccharide-Induced Inflammation-Associated Genes in Macro-Phage Cells via Suppression of NF-κB Signaling Pathway. *Plants* **2023**, *12*, 1241.
(53) Linghu, K.; Lin, D.; Yang, H.; Xu, Y.; Zhang, Y.; Tao, L.; Chen, Y.; Shen, X. Ameliorating effects of 1,8-cineole on LPS-induced human umbilical vein endothelial cell injury by suppressing NF-κB signaling in vitro. *Eur. J. Pharmacol.* **2016**, *789*, 195−201.
(54) Oh, Y. T.; Lee, J. Y.; Lee, J.; Kim, H.; Yoon, K.-S.; Choe, W.; Kang, I. Oleic acid reduces lipopolysaccharide-induced expression of iNOS and COX-2 in BV2 murine microglial cells: Possible involvement of reactive oxygen species, p38 MAPK, and IKK/NF-κB signaling pathways. *Neurosci. Lett.* **2009**, *464*, 93−97.
(55) Yang, I. J.; Lee, D.-U.; Shin, H. M. Inhibitory Effect of Valencene on the Development of Atopic Dermatitis-Like Skin Lesions in NC/Nga Mice. *Evidence-Based Complementary Altern. Med.* **2016**, *2016*, No. 9370893.
(56) Sandilands, A.; Sutherland, C.; Irvine, A. D.; McLean, W. H. Filaggrin in the frontline: role in skin barrier function and disease. *J. Cell Sci.* **2009**, *122*, 1285−1294.
(57) van Mierlo, M. M. F.; Caspers, P. J.; Jansen, M. S.; Puppels, G. J.; Nouwen, A. E. M.; Bronner, M. B.; Pardo, L. M.; van Geel, M.; Pasmans, S. Natural moisturizing factor as a biomarker for filaggrin mutation status in a multi-ethnic paediatric atopic dermatitis cohort. *Clin. Exp. Allergy* **2021**, *51*, 1510−1513.
(58) Páyer, E.; Szabo-Papp, J.; Szabó-Papp, J.; Ambrus, L.; Szöllősi, A. G.; Andrási, M.; Dikstein, S.; Kemény, L.; Juhász, I.; Szegedi, A.; Bíró, T. Beyond the physico-chemical barrier: Glycerol and xylitol markedly yet differentially alter gene expression profiles and modify signalling pathways in human epidermal keratinocytes. *Exp. Dermatol.* **2018**, *27*, 280−284.
(59) Kim, K.-P.; Jeon, S.; Kim, M.-J.; Cho, Y. Borage oil restores acidic skin pH by up-regulating the activity or expression of filaggrin and enzymes involved in epidermal lactate, free fatty acid, and acidic free amino acid metabolism in essential fatty acid-deficient Guinea pigs. *Nutr. Res.* **2018**, *58*, 26−35.
(60) Boskou, D.; Blekas, G.; Tsimidou, M. 4-Olive Oil Composition. In *Olive Oil*, 2nd ed.; Boskou, D., Ed.; AOCS Press, 2006; pp 41−72.
(61) Lammari, N.; Louaer, O.; Meniai, A. H.; Elaissari, A. Encapsulation of Essential Oils via Nanoprecipitation Process: Overview, Progress, Challenges and Prospects. *Pharmaceutics* **2020**, *12*, 431.
(62) Desbois, A. P.; Smith, V. J. Antibacterial free fatty acids: activities, mechanisms of action and biotechnological potential. *Appl. Microbiol. Biotechnol.* **2010**, *85*, 1629−1642.